RESEARCH ON TEMPERATURE RISE CALCULATION AND HOT SPOT TEMPERATURE INVERSION METHOD FOR OIL IMMERSED TRANSFORMER BASED ON MAGNETIC-THERMAL-FLUID

by

FaTing YUAN[a,b*], NaiYue ZHANG[a], WenYu SHI[a], LingYun GU[c], JiHao ZENG[a], and Bo TANG[a,b]

[a] College of Electrical Engineering and New Energy, China Three Gorges University, Yichang, China
[b] Hubei Provincial Engineering Technology Research Center for Power Transmission-Line, China Three Gorges University, Yichang, China
[c] Beijing Key Laboratory of Distribution Transformer Energy-Saving Technology (China Electric Power Research Institute), Beijing, China

Original scientific paper
https://doi.org/10.2298/TSCI231120063Y

The hot spot temperature of oil-immersed transformer winding is an important factor affecting the aging of material insulation. In this paper, a magnetic field simulation model is established based on the electrical and structural parameters of the oil-immersed transformer, and the loss distribution characteristics of each wall of the transformer core, winding and fuel tank are accurately calculated by using the finite element simulation software. The simulation model of transformer fluid-thermal field is established, the simulation results of transformer thermal field are obtained, and the temperature distribution of oil-immersed transformer core and winding and the flow velocity around it are obtained. According to the simulation results of thermal field, the characteristic temperature measuring points with strong correlation between tank wall and winding temperature were determined. The inversion models of tank wall and winding hot spot temperature were established by using the support vector regression and back propagation neural network algorithm, respectively by central composite design method. The results show that the correlation coefficient of support vector regression algorithm in predicting winding hot spot temperature reaches 0.98, and the relative error between the model predicted value and the real value is less than 8%, which is more accurate than back propagation neural network. The aforementioned research provides the theoretical basis and technical support for real-time monitoring of oil-immersed transformer winding hot spot temperature.

Key words: *oil-immersed transformer, support vector regression, back propagation neural network, hot spot temperature*

Introduction

As the key equipment of distribution system, oil-immersed transformer plays an important role in voltage transformation and power distribution. The heat generated during the operation of the transformer will increase the internal temperature of the transformer and cause equipment damage. The heat generated by the transformer comes from the loss of the internal structural parts. The loss of the transformer cannot be accurately calculated, the overall temperature distribution of the transformer and the hot spot temperature of the winding cannot

* Corresponding author, e-mail: yuanfatinghss@163.com

be accurately obtained, which will have a certain impact on the subsequent inversion of the winding temperature. Therefore, the accurate calculation of the loss temperature rise of each transformer component is the key to ensure the safe and reliable operation of the transformer and improve the reliability rate of the power grid. At present, the surface impedance method and traditional finite element method are usually used to calculate the loss temperature rise of oil-immersed transformers [1]. Zhao and Wen [2], the surface impedance method is used to calculate the depth of stray losses such as transformer oil tank, iron core and pull plate, so as to effectively calculate transformer eddy current loss and hysteresis loss. Huang *et al*. [3], the field-route coupling method was used to conduct finite element calculation of the tank eddy current loss, analyze the simulation value of the loss, as well as the distribution of the tank surface magnetic flux density and eddy current loss. Jiang and Lin [4] uses the traditional finite element method and surface impedance method to calculate the eddy current loss on the transformer core clamp. The eddy current density distribution obtained by the two modelling methods is compared and analyzed, and the accuracy of the surface impedance method to calculate the eddy current distribution on the conductor surface is verified. Yuan *et al*. [5] uses a multi physical field simulation analysis method to obtain the temperature and oil flow velocity distribution of transformers. Zao and Wen [6] simulates the 3-D electromagnetic field based on the finite element method, and the calculated results are coupled to the thermal field, and the hot spot temperature of the transformer winding is further predicted. Chen *et al*. [7] proposes an equivalent method for transformer boundary radiation convection composite heat transfer based on mathematical description of heat transfer. Laidoudi *et al.* [8] determines the percentage of heat energy transferred between the nanofluid and the bottom wall of the container under the influence of a set of criteria. Herouz *et al*. [9] studies the MHD mixed convection of nano-encapsulated phase change material (NEPCM) in a hexagonal porous cavity in contact with a square obstacle. Younis *et al*. [10] attempts to improve the thermal characteristics of NEPCM for heating and cooling applications. Younis *et al*. [11] uses Galerkin finite element method to numerically solve the governing equation and discusses the influence of heat transfer factors on heat transfer rate. Laidoudi and Chibanin [12] studies the rheological properties of fluids by changing the value of the power law index, and proves that the thermal activity of different objects is different. The aforementioned literature involves the application of surface impedance method in calculating losses, but most of them only focus on eddy current loss calculation, which cannot guarantee the accuracy of the simulation results of transformer thermal field. In the calculation of thermal field, the simplified model of transformer is used, which is difficult to accurately reflect the distribution of transformer thermal field.

In order to obtain the winding hot spot temperature of oil-immersed transformer, the hot spot temperature inversion research is carried out after analyzing the whole temperature distribution of transformer accurately. At present, the hot spot temperature calculation methods of oil-immersed transformers at home and abroad are mainly divided into four categories: the multi-physical modelling calculation method, empirical formula method, artificial intelligence algorithm and hot path model method. Ni *et al*. [13] extracts typical flow lines between the winding hot spot area and the shell heat dissipation area, selects characteristic temperature measurement points with strong correlation, and establishes a hot spot temperature inversion model. Duan *et al*. [14] uses multi-physical field simulation technology to extract characteristic variables such as environmental temperature, top oil temperature, and load coefficient, and adopts back propagation neural network to establish the inversion model of transformer hot spot temperature. Li *et al*. [15] applied the support vector regression machine to predict hot spot temperature using six characteristic variables such as transformer load current and ambient temperature. The aforementioned literature can all invert the temperature of winding hot spots. However, the selection of temperature points for these existing literature features is relatively blind, and the accuracy of inversion cannot be guaranteed.

In this paper, the loss calculation module in the finite element software is used to calculate each wall surface of the fuel tank based on the magnetic-thermal-fluid multi-physical field simulation analysis, and the overall temperature distribution of the oil-immersed transformer can be further obtained with higher accuracy. According to the simulation results of the temperature of the oil tank, the characteristic points were found, and six characteristic values, namely transformer core loss, winding loss, tank wall loss, ambient temperature, tank heat transfer coefficient and heat sink heat transfer coefficient, were taken as influencing factors. BP back propagation neural network algorithm and support vector regression algorithm were used to invert the hot spot temperature of the transformer winding, and the inversion accuracy of the model was demonstrated, which can be better applied to engineering practice.

The basic structure and equivalent model of transformer

The basic structure and parameters of transformer

The research object of this article is a three-phase oil-immersed transformer, and its main electrical parameters are shown in tab. 1. The iron core of the transformer is composed of cold-rolled silicon steel sheets stacked together, and the windings are divided into high voltage, medium voltage, and low voltage windings. The oil tank is filled with transformer oil, mainly for heat transfer. The chip type heat dissipation fins form the heat dissipation system of the transformer, achieving natural circulation cooling of oil, fig. 1.

Table 1. Main electrical parameters of transformers

Parameter	Value (Model)
Model	OSFSZ10-240000/220/115/37
Rated capacity	240000 kVA
Rated frequency	50 Hz
Connection group	Dyn11
Cooling method	SFSZ
Rated voltage	220 kV

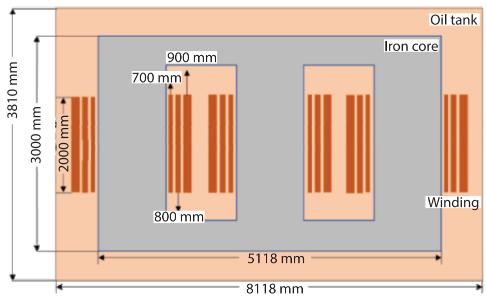

Figure 1. Physical architecture of the model

Transformer equivalent model

The oil tank, iron core, and winding are important components of the transformer's functional and structural support. 3-D equivalent modelling of the transformer is carried out using simulation software based on the actual structural parameters of the transformer. Considering the influence of the internal structure of the oil immersed transformer on the calculation, the model is simplified:

– It is approximately assumed that the resistivity and permeability of the oil tank material are constants.
– Neglecting the losses generated in structural components such as clamps and pull plates, the heat source is mainly the losses of the iron core, winding, and oil tank.
– There is no direct oil passage between the inner and outer cylinders of the low voltage winding.

– It is approximately believed that the oil tank is symmetrical in terms of the three-phase winding connection from top to bottom and from front to back.

The 3-D equivalent model and internal structure of the transformer are shown in figs. 2(a) and 2(b). The winding coils are divided into A, B, and C three-phase.

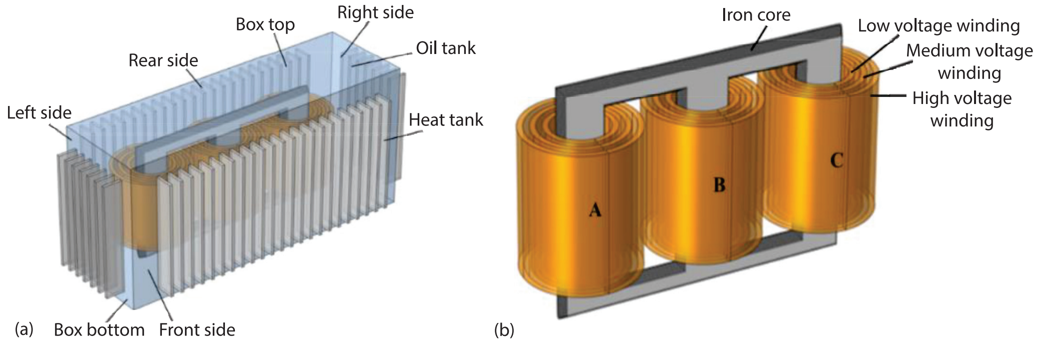

Figure 2. (a) Transformer model diagram and (b) internal structure of transformer

Magnetic field simulation calculation

When the load current flows through the transformer, in addition the main magnetic flux generated through the iron core and winding, there is a small amount of leakage magnetic flux through the oil, whose calculation satisfies the basic equation of the electromagnetic field.

Basic theory of loss calculation

In order to obtain the loss distribution of each component of the transformer under rated load, the rated current applied by the high voltage, medium voltage and low voltage windings of the winding coil is 3958.9 A, 1204.9 A, and 602.5 A, respectively. The loss of iron core is calculated based on the finite element simulation software. The Steinmetz formula [16], which is the most widely used in engineering:

$$Q_c = \kappa_h f^{\alpha} B_m^{\beta} \tag{1}$$

where Q_c is the core loss density, f – the frequency of the excitation signal, B_m – the peak magnetic induction intensity, κ_h, α, β are the loss coefficients.

Considering only the resistance loss and ignoring the eddy current loss caused by leakage flux, the calculation formula for the resistance loss of the winding [17]:

$$Q_i = I_i^2 \frac{\pi D_i W_i}{K S_i} \tag{2}$$

where Q_i is the winding loss density of the i^{th} encapsulation, I_i, D_i, W_i, and S_i are the i^{th} encapsulation current, diameter, turns, and cross-sectional area of the wire, respectively, and K – the conductivity of the metal conductor.

Boundary condition setting and meshing

When using the finite element method to calculate the eddy current loss of the transformer oil tank, due to the large volume of the transformer oil tank and the relatively small thickness of the oil tank wall, taking the surface of the tank as the boundary condition solve the magnetic field can simplify the calculation process and save the calculation time. When the frequency of the magnetic field is calculated based on the power frequency of 50 Hz, it can be calculated from the penetration formula [18], and the penetration depth of the oil tank is 1.345 mm. The transformer tank and heat sink are meshed, and the tank surface, as the boundary-layer of magnetic field, needs to be further refined.

Magnetic field simulation calculation results

– Distribution results of magnetic flux density of iron core and winding

For the iron core, a portion of the leakage magnetic flux generated by the winding during transformer operation will pass through the iron core column, while the B-phase iron core column is in the middle position and is greatly affected by the leakage magnetic flux, resulting in a higher magnetic flux density of the B-phase iron core column compared to other two-phases. The highest magnetic flux density is located at the corners of both ends of the B-phase iron core. When conducting magnetic field simulation calculations, set a cycle time of 0.02 seconds to obtain the magnetic flux density distribution of the iron core, winding, and oil tank at 0.015 seconds.

The magnetic flux density distribution of the winding is shown in figs. 3(a) and 3(b). The low voltage winding of the B-phase coil has a higher magnetic flux density, with a maximum magnetic flux density of 0.39 T.

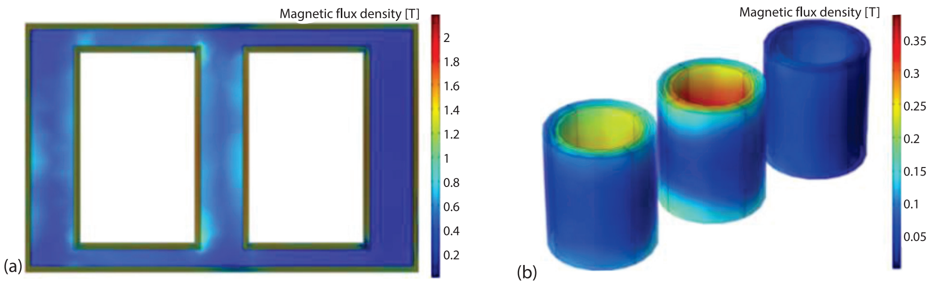

Figure 3. (a) Core flux density distribution and (b) winding flux density distribution

– Result of magnetic flux density distribution on the fuel tank wall

Using the finite element method, the distribution of magnetic flux density on each wall of transformer tank is calculated.

In fig. 4 (a), it can be seen that the magnetic flux distribution on the left wall of the fuel tank is significantly higher than that on the right wall, and its magnetic flux density distribution is basically consistent with that of the winding. As the distance between the coil and the oil tank wall increases, the magnetic flux density on the oil tank wall decreases. Through the analysis of the magnetic flux density on the right wall, it can be seen that the magnetic flux density distribution is more obvious near both ends of the oil tank wall. For the top and bottom of the tank, the magnetic flux density is relatively high near the A-phase and B-phase two-phase coils on the tank wall, and the distribution is basically consistent and for the front and rear wall surfaces, the magnetic flux density is more significant at the left one-third of the two wall surfaces.

Simulation and analysis of transformer flow field temperature field coupling

Loss calculation

According to the calculation formula for core and winding losses mentioned in section *Basic theory of loss calculation*, the final calculation results of core and winding losses are obtained by assigning parameters, as shown in tab. 2.

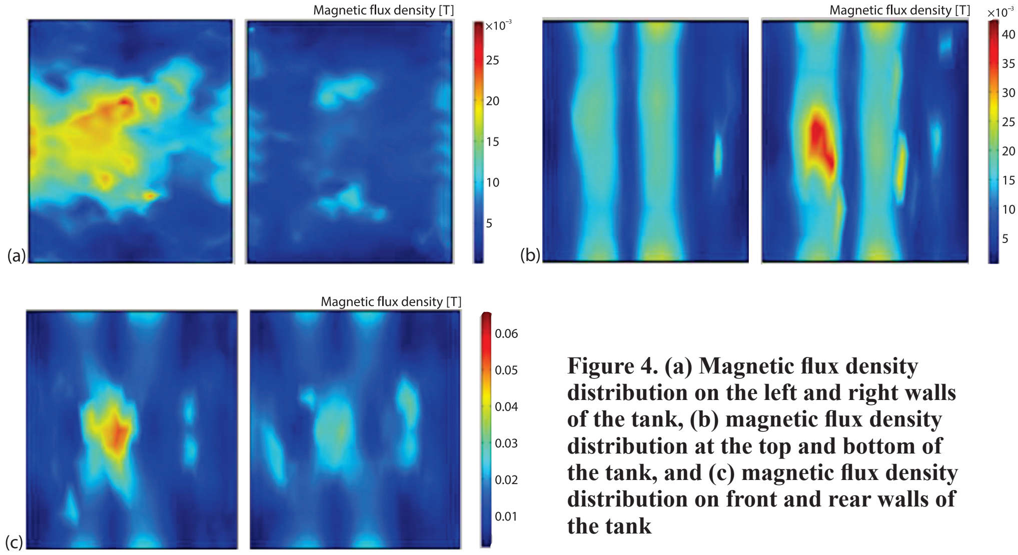

Figure 4. (a) Magnetic flux density distribution on the left and right walls of the tank, (b) magnetic flux density distribution at the top and bottom of the tank, and (c) magnetic flux density distribution on front and rear walls of the tank

Table 2. Distribution of core and winding losses

Part	Loss value [W]
Iron core	35777
Low voltage winding	326104
Medium voltage winding	118601
High voltage winding	67783

The volume loss density reflects the average heating power during the cycle. The loss density distribution of the iron core and winding can be obtained based on the aforementioned calculation results.

In figs. 5(a) and 5(b), it can be seen that the loss density of the core B-phase core column is relatively high, with the highest loss density of $7.29 \cdot 10^9$ W/m^3. The loss density of the B-phase coil is higher than that of the other two-phases, which is basically consistent with the distribution of magnetic flux density in section 3.3 of the winding. The highest loss density of the B-phase coil is $1.06 \cdot 10^8$ W/m^3.

In order to analyze the eddy current losses formed on the transformer oil tank, this paper uses finite element simulation software to calculate the losses on the top, bottom, front, rear, left, and right walls of the transformer oil tank. The loss density distribution results of each wall are shown as follows.

In fig. 6 (a), it can be seen that the loss density on the left wall of the oil tank is significantly higher than that on the right wall. The eddy current loss formed by the winding leakage flux on the left wall of the oil tank is greater, and the maximum loss density is located in the middle of the wall. The distribution of loss density at the top and bottom of the transformer oil tank is basically consistent, and the loss density at the bottom of the oil tank will be slightly higher than that at the top of the oil tank; the trend of loss density on the front and rear walls is basically consistent.

According to the distribution of loss density on each wall of the oil tank, the calculated loss values for each wall are shown in tab. 3.

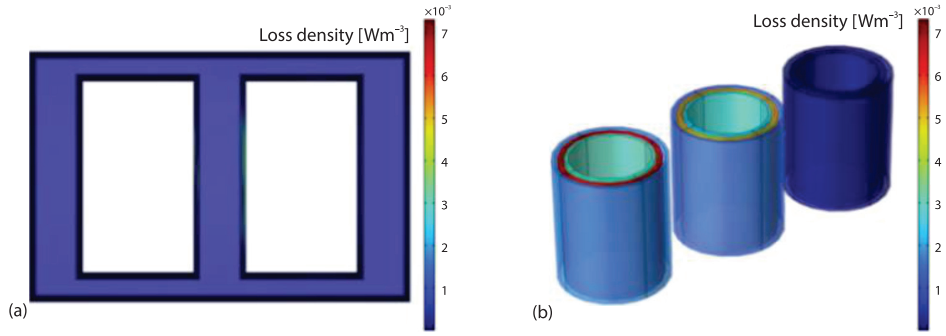

Figure 5. (a) Iron core loss density distribution and (b) winding loss density distribution

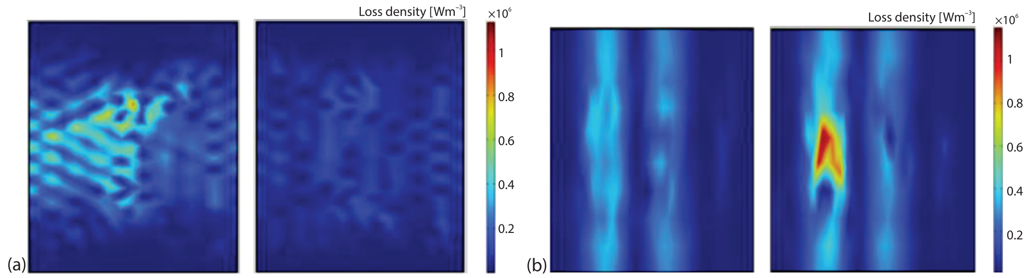

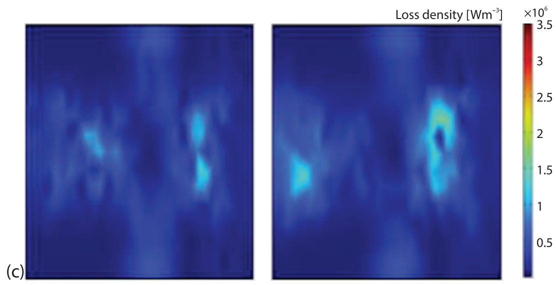

Figure 6. (a) The loss density distribution on the left and right side of the tank, (b) the loss density distribution at the top and bottom of the tank, and (c) the loss density distribution on front and rear walls of the tank

Table 3. Distribution of tank wall loss

Part	Loss value [W]
Left side oil tank wall	29698
Right side oil tank wall	3625
Front oil tank wall	64444
Rear side oil tank wall	63451
Oil tank top	15916
Oil tank bottom	13395
Total oil tank loss	190529

Analysis of transformer heat transfer process

During the actual operation of the transformer, heat is generated inside and transferred to the outside air by convection heat transfer. The heat transfer process of an oil immersed transformer is shown in fig. 7.

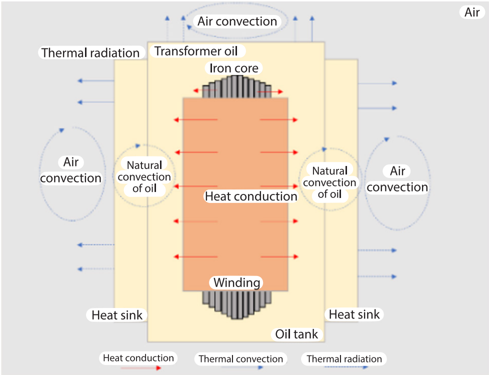

Figure 7. Heat transfer process of oil immersed transformer

Governing equation

For transformers with oil circulation and heat dissipation, the transfer of heat inside the transformer is achieved by the transformer oil. The solution of the convective heat transfer process follows the three fundamental principles of mass conservation, momentum conservation, and energy conservation [19]. The control equation for transformer flow thermal coupling calculation:

$$\vec{q} = -k\nabla T \tag{3}$$

$$\rho C_p \vec{v} T + \nabla \vec{q} = Q \tag{4}$$

$$\frac{\partial \rho}{\partial t} + \nabla(\rho \vec{v}) = 0 \tag{5}$$

where $\vec{q}$ is the vector of heat conduction flux, k – the thermal conductivity, ∇ – the Hamiltonian operator, T – the temperature, ρ [kgm^{-3}] – the fluid density, $\vec{v}$ – the velocity vector, C_p – the constant pressure heat capacity, and Q – the total heat source.

Material property settings

In the simulation of transformer thermal field, it is necessary to set the winding metal conductor, iron core material and flow parameters [4]. The material property settings are shown in tab. 4.

Table 4. Material property settings

Material	Features	Value
Winding (Cu)	Thermal conductivity [Wm^{-1}K^{-1}]	400
	Specific heat volume [Jkg^{-1}K^{-1}]	385
	Density [kgm^{-3}]	8940
Iron core (silicon steel)	Thermal conductivity [Wm^{-1}K^{-1}]	72
	Specific heat volume [Jkg^{-1}K^{-1}]	446
	Density [kgm^{-3}]	7550
Transformer oil	Thermal conductivity [Wm^{-1}K^{-1}]	$0.134\text{-}8.05 \cdot 10^{-5}T$
	Specific heat volume [Jkg^{-1}K^{-1}]	$-13408.15 + 123.04T - 0.33T^2$
	Density [kgm^{-3}]	$1055.05 - 0.58T - 6.4 \cdot 10^{-5}T^2$
	Dynamic viscosity [Pa·s]	$91.45 - 1.33T + 7.78 \cdot 10^{-3}T^2 - 2.27 \cdot 10^{-5}T^3$

Boundary condition setting

At the junction of transformer oil and oil tank wall, it is considered that the fluid near the wall is relatively stationary relative to the wall, that is, the relative velocity of the oil flow near the oil tank wall is zero, and there is no slip on the wall. Set the initial temperature T_0, the ambient temperature is 20 °C. The boundary conditions are shown in fig. 8.

Simulation calculation results

– Thermal field simulation results

Taking the loss density of the transformer core, winding and oil tank as the heat source, the overall temperature and flow velocity distribution of the transformer can be obtained through simulation calculation. The hot spot temperature of the transformer is 64.41 °C, and the temperature rise is 44.41 °C.

According to the simulation results of transformer thermal field, the temperature distribution of iron core and winding is extracted.

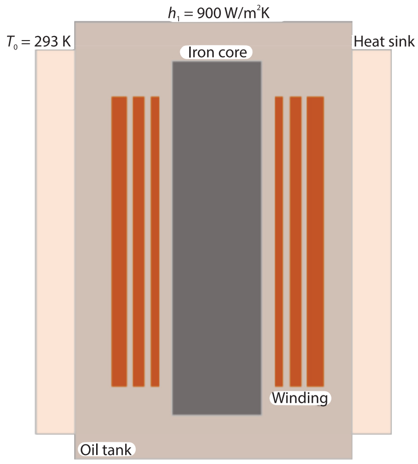

Figure 8. Schematic diagram of boundary conditions

As shown in fig. 9(a), the highest temperature of the iron core is 59.57 °C, with a temperature rise of 39.57 °C, located at the center of the B-phase core column. For the winding, the overall temperature distribution of the low voltage winding is the highest, with the B-phase coil having a slightly higher temperature. The overall temperature of the high voltage winding is relatively low, and the overall temperature of the A-phase coil is slightly lower than that of the other two phases. The heat generated by the iron core and winding is transferred to the transformer oil, and the oil temperature rises and flows upwards. It flows through the oil tank wall and conducts convective heat exchange with the air, causing the highest temperature of the low voltage winding to be in the upper part of the B-phase coil, and the end temperature of the winding to be lower. Considering that the low voltage winding is located on the innermost side of the three windings, the heat dissipation effect is poor, resulting in the highest overall temperature rise of the low voltage winding ultimately.

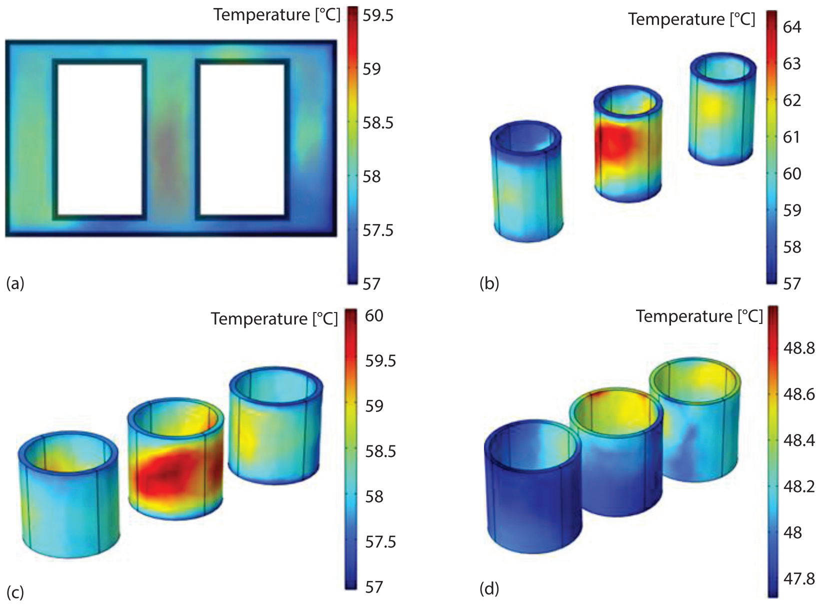

Figure 9. (a) Temperature distribution of iron core, (b) temperature distribution of low voltage winding, (c) temperature distribution of medium voltage winding, and (d) temperature distribution of high voltage winding

In order to better analyze the flow and heat transfer of transformer oil, the simulation results of transformer temperature and oil flow distribution are calculated. According to the overall temperature distribution of the transformer oil tank, it can be seen that the surface temperature of the oil tank is significantly higher than the temperature of the heat dissipation fins. The temperature of the top and bottom areas of the tank is higher, and the temperature of the surrounding wall and heat dissipation fin connection area is lower. The transformer oil transfers heat to the outside through the heat dissipation fins, and the temperature of the heat dissipation fins shows an uneven distribution, fig. 10.

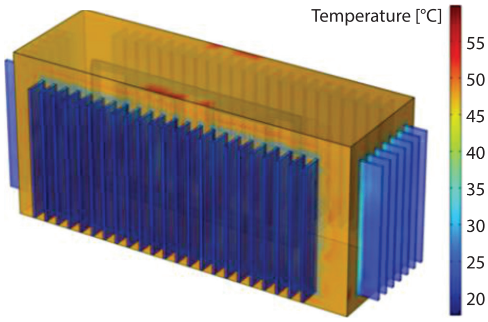

Figure 10. Overall temperature distribution of transformer oil tank

– Fluid field simulation results and analysis

The simulation results of the transformer fluid field are obtained through simulation solution. The overall oil flow velocity distribution is shown in fig. 11. The maximum oil flow velocity is 0.78 m/s, and the highest oil flow velocity is located near the B and C phase coils, with obvious eddy current phenomenon. After the iron core and winding generate heat, the transformer oil is heated and flows upward, forming part of the eddy current in the middle and upper part of the tank, flowing through the tank wall and heat sink, and returning to the bottom of the tank after cooling to achieve circulation flow inside the transformer.

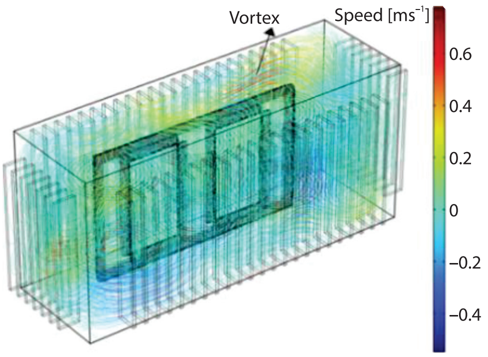

Figure 11. Distribution of transformer oil flow velocity

Mesh independence study

At the same time, mesh independence study is carried out, and hot spot temperatures with different numbers of meshes are given in tab. 5. It can be inferred that when the number of nodes is 898749, the temperature rise reaches a stable value.

Table 5. The hot spot temperature under different meshes

Number of nodes	210513	304582	470250	898749
T_{max} [°C]	63.88	64.13	64.40	64.41

Transformer hot spot temperature inversion model

Transformer hot spot temperature inversion method based on back propagation neural network

The back propagation neural network algorithm

The back propagation neural network is a multi-layer feedforward neural network learning algorithm. Back propagation neural network is a hierarchical neural network composed of input layer, intermediate layer and output layer. The intermediate layer can be extended to multiple layers, and each layer can have several nodes. The nodes between adjacent layers are fully connected, while the nodes of each layer are not connected, and the connection status between layers is reflected by the weight. The main characteristics of back propagation neural network are forward propagation of signal and back propagation of error, fig. 12. In forward transmission, the input signal is processed layer by layer from the input layer through the middle layer until the output layer. The node status of each layer affects only the node status of the next layer. If the output layer does not get the expected output, it turns to back propagation, and adjusts the weight and threshold according to the prediction error constantly, so that the back propagation neural network predicts the output error constantly tends to the given minimum value, that is, the learning process is completed. The total number of experimental design samples in this paper is 86. Through the continuous learning of 86 groups of data in the back propagation neural network code program written in MATLAB, the algorithm can complete the learning after the 10th iteration.

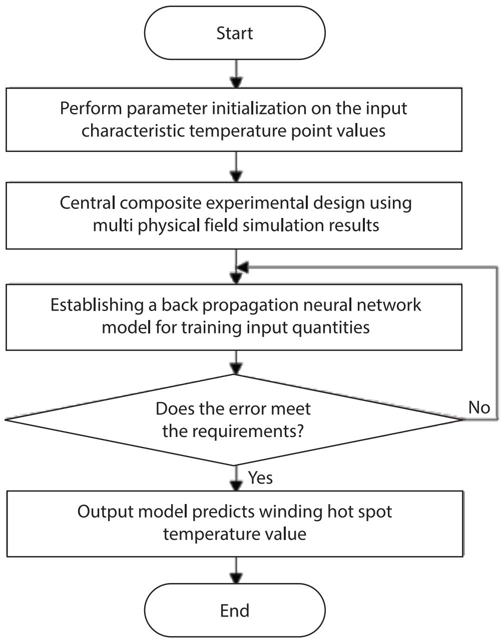

Figure 12. Core steps of neural network

Central composite experimental design

Central composite design is a widely used experimental design method, which can greatly reduce the number of experiments and the time required for simulation. The hot spot temperature of the transformer is taken as the output target of the back propagation neural network algorithm, and the temperature of the upper and lower dead corners of the oil tank and the ambient temperature listed in [20] are used as temperature characteristic variables. Deng *et al.* [21] considers the influence of boundary conditions on the thermal field distribution of the transformer, and selects low voltage heat source power, high voltage heat source power, and convective heat transfer coefficient as temperature characteristic variables. This article ultimately selects six proportional coefficients as factor levels based on the selection results of the aforementioned temperature characteristic variables: the convective heat transfer coefficient, h_1, of the transformer oil tank, the convective heat transfer coefficient, h_2, of the transformer heat sink, the ambient temperature, T, the iron core loss, Q_c, the winding loss, Q_i, and the oil tank loss, Q_w. Establish a factor level table with six factors and five levels, as shown in tab. 6.

Table 6. Factor level table

Factor level	Experimental factors					
	h_1	h_2	T	Q_c	Q_i	Q_w
1	600.00	900.00	10.00	0.90	0.90	0.90
2	636.10	936.10	13.61	0.93	0.93	0.93
3	700.00	1000.00	20.00	1.00	1.00	1.00
4	763.89	1063.89	26.39	1.06	1.06	1.06
5	800.00	1100.00	30.00	1.10	1.10	1.10

The feature points select of transformer

According to the analysis of the temperature of transformer oil tank, the characteristic temperature points of transformer are selected for simulation calculation, and the hot spot temperature inversion is carried out by using BP neural network. The characteristic temperature points selected in [19], and the hot spot temperature obtained by simulation in section *Simulation calculation results* are distributed in the middle and upper 2/3 of the winding, as shown in fig. 13(a). Finally, a total of 10 temperature measurement points were selected for temperature inversion, including corresponding points of three-phase windings A, B, and C at the middle and upper 2/3 height of the oil tank, corresponding points of three-phase windings A, B, and C at the top of the oil tank, heat sink and corners. The distribution of 10 feature points is shown in fig. 13(b).

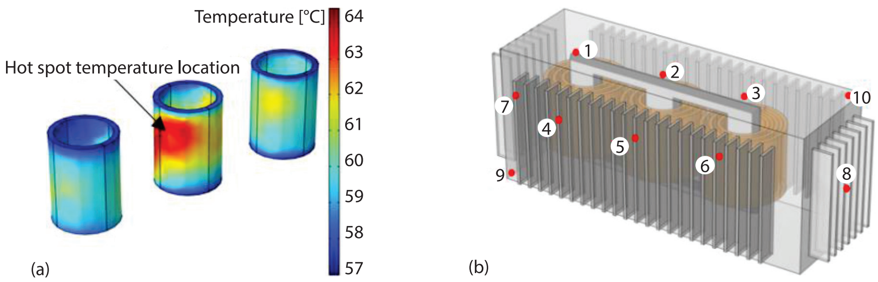

Figure 13. (a) Hot spot temperature distribution and (b) feature point selection

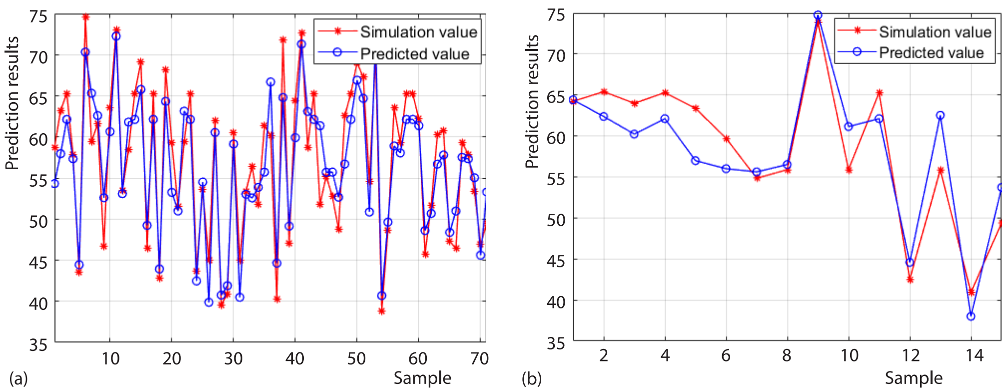

Figure 14. (a) Training set result and (b) test set result

Hot spot temperature inversion results and analysis

The hot spot temperature inversion model for oil immersed transformers based on back propagation neural network uses the temperature data of each characteristic point on the transformer oil tank wall obtained in section *The feature points select of transformer* as input and the hot spot temperature as output. The total number of samples is 86 groups. Divide the distribution of training and testing sets approximately into 80% and 20%. The back propagation neural network is trained by randomly selecting samples. The comparison between the training set and the test set and the predicted values is shown in figs. 14(a) and 14(b). After calculation, the maximum relative error between the training set and simulation values is 0.094, and the maximum relative error between the test set and simulation values is –0.111.

The back propagation neural network algorithm is used to predict the samples, and finally the correlation coefficient R^2 of back propagation neural network model is 0.87.

Transformer hot spot temperature inversion method based on support vector machine

Support vector regression algorithm

Support vector machine is a modelling method based on small sample statistical learning theory and structural risk minimization. It establishes a hyperplane by providing a set of sample training sets to describe the multi-dimensional non-linear relationship between the input quantity x and the output target y, that is, $f(x) = \omega x + b$, and $f(x)$ satisfies the relationship:

$$|y_i - f(x)| \le \varepsilon, \quad i = 1, 2, ... \tag{6}$$

where x_i is the i^{th} input vector, y_i – the i^{th} output parameter, and ε – the insensitive loss coefficient.

For any point (x_i, y_i) in the training set, the distance d_i from that point to the hyperplane can be represented:

$$d_i = \frac{|\omega x_i + b - y_i|}{\sqrt{1 + \|\omega\|^2}} \le \frac{\varepsilon}{\sqrt{1 + \|\omega\|^2}}, \quad i = 1, 2, ..., N \tag{7}$$

A hyperplane that minimizes the distance between all training sample sets and the plane is found, this plane is the optimal hyperplane.

The solution the optimal hyperplane problem can be expressed:

$$\begin{gathered} \min \varphi(\omega) = \frac{1}{2}\|\omega\|^2 \\ s.t. |\omega x_i + b - y_i| \le \varepsilon, \quad i = 1, 2, ... N \end{gathered} \tag{8}$$

Support vector regression hot spot temperature inversion model

The support vector regression requires fewer samples for prediction, and the selection of samples is more regular compared to back propagation neural networks, resulting in higher prediction accuracy. The comparison of the 10 feature point prediction training set and test set with the predicted value is shown in figs. 15(a) and 15(b).

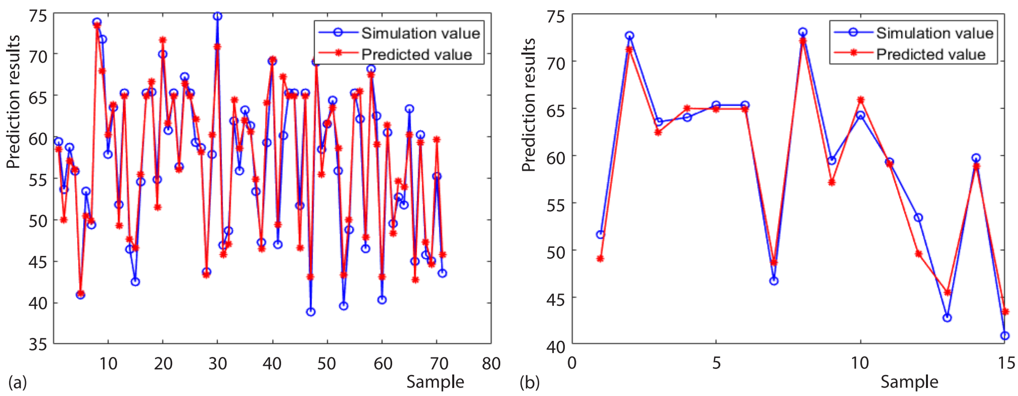

Figure 15. (a) Training set result and (b) test set result

The correlation coefficient of the support vector machine prediction model reaches above 0.98, it shows that the support vector machine prediction model has higher accuracy in predicting the hot spot temperature of transformer winding.

The support vector machine inversion model was used to perform hot spot temperature inversion on 10 feature points, and the inversion results of the test set are shown in tab. 7.

Table 7. Comparison of simulation and prediction values of support vector machine test set

Sample	Simulation value [°C]	Predicted value [°C]	Temperature difference [°C]	Relative error
1	51.58	48.99	2.59	0.050
2	72.65	71.18	1.47	0.020
3	63.52	62.42	1.1	0.017
4	63.98	64.95	–0.97	–0.015
5	65.29	64.89	0.40	0.006
6	65.29	64.89	0.40	0.006
7	46.67	48.61	–1.94	–0.042
8	73.04	72.14	0.90	0.012
9	59.42	57.09	2.33	0.039
10	64.22	65.88	–1.66	–0.026
11	59.27	59.02	0.25	0.004
12	53.38	49.56	3.82	0.072
13	42.77	45.47	–2.7	–0.063
14	59.71	58.87	0.84	0.014
15	40.88	43.46	–2.58	–0.063

According to the tab. 6, the maximum relative error between the training set and the simulation value using support vector machine inversion model is –0.117, and the maximum relative error between the test set and the simulation value is 0.071. The relative error of all 15 test samples is less than 8%.

Result analysis

Performance evaluation indicators

Error analysis is one of the important steps in transformer temperature inversion. It is possible to better scientifically evaluate the advantages and disadvantages of inversion models by error analysis. This article evaluates the predictive performance of the prediction model by predicting all samples using root mean square error (RMSE), mean absolute error (MAE), and correlation coefficient, R^2. The expressions of each evaluation index are shown:

$$\text{RMSE} = \sqrt{\frac{1}{k}\sum_{j=1}^{k}\left(\hat{y}_j - y_j\right)^2} \tag{9}$$

$$\text{MAE} = \frac{1}{k}\sum_{j=1}^{k}\left|\hat{y}_j - y_j\right| \tag{10}$$

$$R^2 = \frac{\sum_{j=1}^{k}\left(\hat{y}_j - \overline{y}\right)^2}{\sum_{j=1}^{k}\left(y_j - \overline{y}\right)^2} \tag{11}$$

The comparison of error evaluation indicators between the two models is shown in tab. 8.

Table 8. Comparison of error evaluation indicators

Error evaluation indicators	RMSE	MAE	R^2
BP neural network	3.64	3.10	0.88
Support vector machine	1.88	1.59	0.98

The error evaluation indicators of the inversion model are given in tab. 8. Among them, the lower the MAE and RMSE, the smaller the error. The closer the R^2 is to 1, the closer it is to the true value, and the more accurate the predicted model results. The RMSE of the back propagation neural network is 3.64, the average absolute error is 3.10, and the correlation coefficient is 0.88. The RMSE of the support vector machine is 1.88, the average absolute error is 1.59, and the correlation coefficient is 0.98. The back propagation neural network temperature inversion model has greater error and the fitting effect is general. The use of support vector machine models can reduce the error of inversion results and make predictions more accurate. Its prediction performance is far better than that of back propagation neural network models, verifying the superiority of support vector regression algorithms in predicting hot spot temperatures. The use of temperature inversion models can monitor and predict the hot spot temperature of transformer winding in real time, saving a lot of labor and financial costs, while ensuring the safe and stable operation of transformers.

Conclusions

Firstly, 3-D equivalent modelling is carried out for the oil-immersed transformer, and accurate loss density distribution of the transformer core, winding and oil tank is obtained from the magnetic field calculation results. The loss density can be substituted into the temperature field calculation as a heat source to obtain a more accurate overall temperature distribution of the transformer.

Secondly, the temperature and flow velocity distribution of the transformer were obtained through flow field temperature field simulation. The hot spot temperature of the transformer was 64.46 °C. Laidoudi *et al*. [22] discusses the effect of thermal buoyancy on the characteristics of convective heat transfer. Houssem [23] and Houssem and Mohamed [24] discusses the effects of natural-convection control parameters, such as Prandtl number and Rayleigh number, on fluid motion and heat transfer rate. Different from previous studies, this paper uses the heat transfer module in the finite element simulation software to directly set the convective heat transfer coefficient, and obtains the maximum oil flow velocity of the transformer as 0.78 m/s. According to the distribution results of the transformer fluid-thermal field,it can be seen that the hot spot of the transformer is located at the upper middle of the low voltage winding B- and C-phase coils. The eddy current phenomenon near the C-phase coils is more obvious due to the higher temperature of the C-phase high voltage winding compared to other two-phase windings.

Finally, according to the simulation distribution results of the transformer fluid-thermal field obtained by our research, a sample database for the temperature of the external characteristic points of the transformer is established, and invert the hot spot temperature of the transformer through support vector regression and neural network algorithms. After comparing various performance evaluation indexes of the two algorithms, and find that the correlation coefficient of the support vector machine model in the inversion prediction is above 0.98, and the relative error between the predicted value of the model and the real value is less than 8%. The prediction performance of support vector regression algorithm is proved to be superior.

Acknowledgment

This work is supported by the National Natural Science Foundation of China（52307179). The Open Fund of Beijing Key Laboratory of Distribution Transformer Energy-Saving Technology (PDB51202301652).

Nomenclature

B_m – peak magnetic induction intensity, [T]
C_p – constant pressure heat capacity, [JKg^{-1}K^{-1}]
D_i – i^{th} diameter of the wire, [mm]
d_i – distance to the hyperplane, [mm]
f – frequency of the excitation signal, [Hz]
I_i – i^{th} encapsulation current of the wire, [A]
K – conductivity of the metal conductor, [Sm^{-1}]
k – thermal conductivity, [Wm^{-1}K^{-1}]
Q – total heat source, [kWh]
Q_c – core loss density, [W]
Q_i – winding loss density of the i^{th} encapsulation, [W]
$\vec{q}$ – vector of heat conduction flux
S_i – i^{th} cross-sectional area of the wire, [mm^2]
T – temperature, [°C]
$\vec{v}$ – velocity vector
W_i – i^{th} turns of the wire
x_i – i^{th} input vector
y_i – i^{th} output parameter

Greek symbols

α, β – loss coefficients
ε – insensitive loss coefficient
∇ – Hamiltonian operator
κ_h – loss coefficients
ρ – fluid density, [kgm^{-3}]
ω – weight of the optimal hyperplane

References

[1] Liu, H, *et al.*, Calculation of Harmonic Losses in Converter Transformer Casing Based on Impedance Boundary Method (in Chinese), *High Voltage Engineering*, *41* (2015), 09, pp. 3171-3176
[2] Zhao, Z. G., Wen, T., The Modelling Method of Local Surface Impedance in the Calculation of Stray Losses in Transformers (in Chinese), *Journal of Electrical Engineering Technology*, *35* (2020), 22, pp. 4699-4708
[3] Huang, T. C., *et al.*,The effect of DC Bias of Converter Transformer on Eddy Current Loss in Oil Tank (in Chinese), *Journal of Electrical Technology*, *38* (2023), 08, pp. 2004-2014
[4] Jiang, Y. Q., Lin, Y. Y., Calculation of Eddy Current Loss in Iron Core Clamps of Power Transformers (in Chinese), *Electrical Technology*, *453* (2017), 08, pp. 25-26
[5] Yuan, F. T., *et al.*, Temperature Characteristic Analysis and Radiator Optimization of Oil Immersed Transformer Based on Multiphysics Simulation (in Chinese), *High Voltage Engineering*, *50* (2023), 1, pp. 221-231
[6] Zhao, Z. G., Wen, T., The Modelling Method of Local Surface Impedance in the Calculation of Stray Losses in Transformers (in Chinese), *Journal of Electrical Engineering Technology*, *35* (2020), 22, pp. 4699-4708
[7] Chen, W. G., *et al.*, Calculation of Winding Temperature Distribution of Oil Immersed Transformer Based on Finite Volume Method (in Chinese), *Power Automation Equipment*, *31* (2021), 06, pp. 23-27
[8] Laidoudi, H., *et al.*, Irreversibility Interpretation and MHD Mixed Convection of Hybrid Nanofluids in a 3-D Heated Lid-Driven Chamber, *Nanomaterials*, *12* (2022), 10, pp. 1747-1747
[9] Herouz, K., *et al.*, Analysis of Nanoencapsulated Phase Change Material Confined in a Double Lid-Driven Hexagonal Porous Chamber with an Obstacle under Magnetic Field, *Journal of Energy Storage*, *61* (2023), 106736

[10] Younis, O., *et al.*, Thermal Pattern of Nanoencapsulated PCM in a Lid-Driven Cavity with Presence of a Heated Body, Magnetic Field and Limited Permeability, *Case Studies in Thermal Engineering*, *50* (2023), 103469

[11] Younis, O., *et al*., Buoyancy-Driven Flow and Thermal Activity of Nanoenhanced Phase Change Material in Inversed U-Shaped Chamber, *Journal of Energy Storage*, *61* (2023), 106705

[12] Laidoudi, H., Chibani, A., Thermal Activity of Hot Bodies Trapped Inside a Moving Chamber with a Complex Fluid under the Influence of MHD and Buoyancy Forces, *Numerical Heat Transfer, Part B: Fundamentals*, *85* (2024), 5, pp. 569-586

[13] Ni, Z. Z., *et al*., Dynamic Inversion Method of Hot Spot Temperature of Oil Immersed Transformer Based on Multiphysics Simulation and Neural Network Algorithm (in Chinese), *High Voltage Engineering*, *49* (2023), 6, pp. 2466-2477

[14] Duan, C. H., *et al*., Research on the Equivalent Method of Boundary Radiation Convection Combined Heat Transfer for Transformer Temperature Field Calculation (in Chinese), *Journal of Electrical Machinery and Control*, *24* (2020), 10, pp. 120-129

[15] Li, Y. C., *et al.*, Research on Support Vector Machine Method for Short Term Load Forecasting (in Chinese), *Chinese Journal of Electrical Engineering*, *6* (2003), pp. 55-59

[16] Chen, B., *et al.*, Model of Harmonic Losses in Windings and Cores of High-Power Intermediate Frequency Three-Phase Transformers (in Chinese), *High Voltage Engineering*, *48* (2022), 08, pp. 3119-3131

[17] Yuan, F. T., Optimization Design of Dry Type Air-Core Reactor Based on Thermal and Magnetic Combination (in Chinese), Ph. D. thesis, Huazhong University of Science and Technology, Wuhan, China, 2018

[18] Du, C., Calculation and Shielding Study of Eddy Current Losses in the Oil Tank Wall of Power Transformers (in Chinese), MSc thesis, Harbin University of Science and Technology, Harbin, China, 2012.

[19] Tao, W. Q., *Numerical Heat Transfer* (in Chinese), 2nd ed., Xi'an Jiaotong University Press, Xi'an, China, 2001

[20] Chen, W. G., *et al*., A Transformer Winding Hot Spot Temperature Prediction Model Based on Genetic Optimization Support Vector Machine (in Chinese), *Journal of Electrical Engineering Technology*, *29* (2014), 01, pp. 44-51

[21] Deng, Y. Q., *et al*., Establishment and Verification of a Hot Spot Temperature Inversion Model for 10 kV Oil Immersed Transformer Windings Based On Streamline Analysis (in Chinese), *Chinese Journal of Electrical Engineering*, *43* (2023), 08, pp. 3191-3204

[22] Laidoudi, H., *et al*., Natural-Convection of Newtonian Fluids between Two Concentric Cylinders of a Special Cross-Sectional Form, *Thermal Science*, *25* (2021), 5B, pp. 3701-3714

[23] Houssem, L., Natural-Convection from Four Circular Cylinders in Across Arrangement within Horizontal Annular Space, *Acta Mechanica et Automatica*, *14* (2020), 2, pp. 98-102

[24] Houssem, L., Mohamed, B., The Effect of Asymmetrically Confined Circular Cylinder and Opposing Buoyancy on Fluid-Flow and Heat Transfer, *Defect and Diffusion Forum*, *374* (2017), Apr., pp. 18-28

Paper submitted: November 20, 2023
Paper revised: January 4, 2024
Paper accepted: January 11, 2024